Title	Diffusion imaging with balanced steady state free precession
Author(s)	Cheung, MM; Wu, EX
Citation	The 34th Annual International Conference of the IEEE Engineering in Medicine and Biology Society (EMBS 2012), San Diego, CA., 28 August-1 September 2012. In IEEE Engineering in Medicine and Biology Society Conference Proceedings, 2012, p. 90-93
Issued Date	2012
URL	http://hdl.handle.net/10722/191624
Rights	IEEE Engineering in Medicine and Biology Society Conference Proceedings. Copyright © Institute of Electrical and Electronics Engineers.

34th Annual International Conference of the IEEE EMBS
San Diego, California USA, 28 August - 1 September, 2012

Diffusion Imaging with Balanced Steady State Free Precession

Matthew M. Cheung, Ed X. Wu*

Abstract—**Balanced steady state free precession (bSSFP) offers high signal efficiency and relative motion insensitivity. In this study, diffusion weighted bSSFP (DW-bSSFP) was introduced by modifying standard bSSFP sequence with two pairs of balanced bipolar diffusion gradients. The diffusion effect was analyzed and described in closed forms. It was found to be coupled to the transverse and longitudinal relaxation, flip angle and spin phase advance per TR. Such coupling was demonstrated in phantom experiment at 7T. Preliminary DW-bSSFP imaging experiment was performed in rat brain *in vivo* for diffusion tensor imaging, yielding parametric maps qualitatively similar to those obtained with an 8-shot DW-EPI protocol. The proposed DW-bSSFP approach can provide a new means of diffusion imaging with high resolution, relative motion insensitivity and short diffusion time. Such approach may lead to improved and new diffusion characterization of neural tissues, abdominal organs, myocardium and musculoskeletal tissues.**

***Index Terms*—diffusion MRI, balanced SSFP, steady state free precession, diffusion time, motion insensitive**

I. INTRODUCTION

Conventional magnetic resonance (MR) diffusion weighted (DW) images are acquired using spin echo (SE) sequences. Fast acquisition methods can be used to minimize the effect of undesirable bulk motion while detecting the effect of diffusion. Echo planar imaging (EPI) offers high acquisition speed and is now routinely employed in diffusion imaging. However, DW-EPI inherently suffers from low spatial resolution and geometric distortions due to field inhomogeneity, susceptibility related off-resonance effects and gradient eddy currents[1].

Steady state free precession (SSFP) presents an alternative for studying diffusion effect. Analytical description of the diffusion effect in DW-SSFP sequences can be complex because the effect of diffusion cannot be decoupled from the relaxation times and flip angle[2, 3]. The effect of diffusion in presence of a constant gradient was first studied using Fourier decomposition and pulsed gradient per TR analytically partition analysis of echo paths[2]. Subsequent studies described the effect of diffusion in presence of a unipolar together with numerical simulations to show the behavior of signal decays for various combinations of relaxation times and flip angles[3].

Recently SSFP with unipolar diffusion gradients was used to perform diffusion imaging with high spatial resolution[4, 5] and information of tissue orientation was utilized for tractography[6]. These studies employed the unbalanced diffusion gradients within each TR and the signal was shown to be more sensitive to diffusion under the same diffusion weighting factor (b-value) computed per TR because the echo signal consists of multiple and long echo paths during which diffusion weighting occurs. However, such sequences were vulnerable to bulk motion artifacts due to relatively long TR. Bipolar diffusion encoding gradients have been introduced to overcome this problem and implemented in SSFP to acquire DW images using the contrast enhanced Fourier acquired steady state (CE-FAST) sequence[7, 8]. In general, these DW-SSFP sequences have yielded promising results in studying diffusion effect despite the complex dependence of signal decay on tissue relaxation times and imaging parameters. However, imaging and diffusion gradients in these sequences were not fully balanced.

In balanced SSFP (bSSFP), all imaging gradients are fully balanced and signals reach a steady state[9]. With advances in gradient hardware and shimming system, bSSFP is now routinely employed in applications that require a rapid and motion insensitive sequence such as cardiovascular imaging and abdominal imaging, and those demanding more isotropic voxels to avoid partial volume effects such as musculoskeletal imaging. So far, there has been no theoretical and experimental attempt to exploring and utilizing the diffusion effect in bSSFP sequence that incorporates balanced bipolar diffusion gradients. Such fully balanced diffusion weighted bSSFP sequence (DW-bSSFP) can retain the advantage of standard bSSFP in achieving high signal efficiency. More importantly, it offers promise of high spatial resolution and minimal image distortion and it is less sensitive to bulk motion because of the very short TR and fully balanced gradients.

This work aimed to formulate the analytical description of diffusion effect in the proposed DW-bSSFP sequence and examine the influence of relaxation times, flip angle and phase advance. The issues related to its practical implementation for diffusion imaging and potential applications were also discussed.

II. MATERIALS AND METHODS

A. Theory

To probe the diffusion effect, two symmetric pairs of bipolar diffusion encoding gradients are introduced per TR in bSSFP as shown in Figs. 1 and 2. Without losing generality, only diffusion gradients along one particular direction are considered together with a series of RF pulses of flip angle α around x-axis with successive phase advance β within each TR (Fig. 1). The overall effect of bipolar diffusion gradient can be considered as an enhanced T_2 effect throughout TR. The transverse magnetization in DW-bSSFP evolves identically to that derived for standard bSSFP imaging

This work was supported in part by the University of Hong Kong CRCG grant and Hong Kong Research Grant Council grant.

Ed X. Wu and Matthew M. Cheung are with the Laboratory of Biomedical Imaging and Signal Processing and the Department of Electrical and Electronic Engineering, The University of Hong Kong, Pokfulam, Hong Kong (phone: (852) 2819-9713; e-mail: ewu@eee.hku.hk).

sequence[2], with enhanced T_2 decay throughout TR. The magnetization immediately after excitation at steady state is:

$$\begin{cases} M_y(0^+) = M_0(1-E_1)\dfrac{\sin\alpha(1-e^{-2bD}E_2\cos\beta)}{(1-E_1\cos\alpha)(1-e^{-2bD}E_2\cos\beta)-e^{-2bD}E_2(E_1-\cos\alpha)(e^{-2bD}E_2-\cos\beta)} \\ M_x(0^+) = M_y(0^+)\dfrac{e^{-2bD}E_2\sin\beta}{1-e^{-2bD}E_2\cos\beta} \end{cases} \quad (1)$$

where $E_1 \equiv e^{-TR/T_1}$ and $E_2 \equiv e^{-TR/T_2}$ and b is the diffusion weighting factor($2\gamma^2G^2\delta^3/3$) . Signal at TE=TR/2 is:

$$\left|M_{xy}(TR/2)\right| = e^{-bD}e^{-TR/2T_2}[M_x^2(0^+)+M_y^2(0^+)]^{1/2}. \quad (2)$$

Eqs. 1 and 2 indicate that the effect of diffusion in DW-bSSFP is related to not only bD but also T_1, T_2, TR, flip angle α and phase advance β. When β=0, the DW signal attenuation can be expressed as

$$\frac{S_{b,\beta=0}}{S_{0,\beta=0}} = \frac{e^{-bD}(1-E_1\cos\alpha+E_1E_2-E_2\cos\alpha)}{(1-E_1\cos\alpha+e^{-2bD}E_1E_2-e^{-2bD}E_2\cos\alpha)} \quad (3),$$

where S_b and S_0 are the signals with and without diffusion weighting, respectively. When β = π, it is

$$\frac{S_{b,\beta=\pi}}{S_{0,\beta=\pi}} = \frac{e^{-bD}(1-E_1\cos\alpha-E_1E_2+E_2\cos\alpha)}{(1-E_1\cos\alpha-e^{-2bD}E_1E_2+e^{-2bD}E_2\cos\alpha)}. \quad (4)$$

In practice, E_1 can be assumed to be unity if TR<<T_1 and Eqs.3 and 4 will then reduce to the following and become independent of flip angle α if α is not very small:

$$\frac{S_{b,\beta=0}}{S_{0,\beta=0}} \approx \frac{e^{-bD}(1+E_2)}{(1+e^{-2bD}E_2)}, \quad (5)$$

$$\frac{S_{b,\beta=\pi}}{S_{0,\beta=\pi}} \approx \frac{e^{-bD}(1-E_2)}{(1-e^{-2bD}E_2)}. \quad (6)$$

In another scenario when the b-value is sufficiently large (2bD>>1) such that the residual transverse magnetization at end of each TR is negligible, the effect of diffusion acts on the DW-bSSFP signal in a monoexponential decay manner, similar (but not identical) to the diffusion effect in the fast low angle shot (FLASH) with bipolar diffusion gradients. In this case, Eqs.3 and 4 reduce to the following and exhibit monoexponential dependence on diffusivity:

$$\frac{S_{b,\beta=0}}{S_{0,\beta=0}} \approx \frac{e^{-bD}(1-E_1\cos\alpha+E_1E_2-E_2\cos\alpha)}{(1-E_1\cos\alpha)}, \quad (7)$$

$$\frac{S_{b,\beta=\pi}}{S_{0,\beta=\pi}} \approx \frac{e^{-bD}(1-E_1\cos\alpha-E_1E_2+E_2\cos\alpha)}{(1-E_1\cos\alpha)}. \quad (8)$$

B. MR acquisition

Preliminary MRI experiments were performed in phantoms and in vivo rat brains using a 7T Bruker PharmaScan MRI scanner with maximum gradient of 360 mT/m. ***Gadolinium phantoms:*** Uniform gel suspensions with different concentrations (0.05 mM, 1 mM, 2.5 mM, 5 mM) of Gadolinium (Gd) (Dotarem®, Guerbet) were prepared in 4-cm long, 1-cm diameter, 2-mL cylindrical phantom tubes. Localized voxel shimming with fast automatic shimming technique mapping along projections (FASTMAP) was performed individually in each phantom before acquiring data. DWIs of the phantoms were acquired using the proposed DW-bSSFP sequence with multiple b-values ranging from 0 to 1000 s/mm^2 applied along the readout direction. The following parameters were used: TR/TE=46/23 ms, δ=10 ms, flip angle α=30°, field of view (FOV)=45X45 mm^2, acquisition matrix=128X128, slice thickness=1 mm and

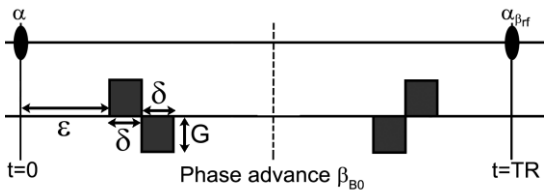

Fig. 1. A simplified balanced steady state free precession (bSSFP) sequence with two pairs of bipolar diffusion encoding gradients of amplitude G and duration δ per TR. The first pair of bipolar gradients begins at time ε after the RF pulse. Dashed line indicates the echo time TE at TR/2.

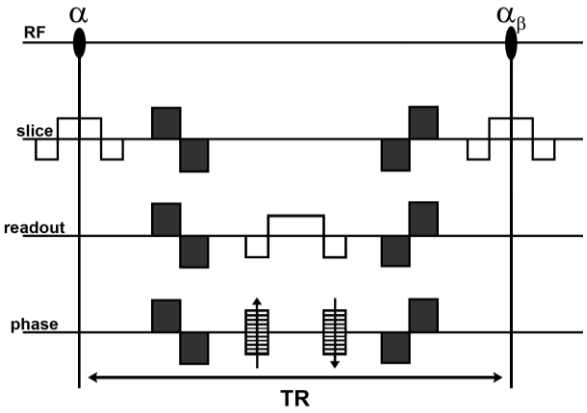

Fig. 2 The proposed diffusion weighted (DW) bSSFP (DW-bSSFP) imaging sequence. Diffusion encoding gradients (solid black areas) can be inserted along slice, readout and phase encoding directions.

number of excitations (NEX)=16. Alternating RF pulses were used (β=π) and the maximum magnitude of the diffusion gradient (G) was 144 mT/m. Large circular regions of interest (ROIs) covering the gels in each Gd phantoms were drawn to measure the DW signal decays. DWIs were also acquired using an 8-shot DW SE-EPI with the TR/TE=3200/28 ms, δ/Δ=5/10 ms, identical b-values, image resolution and slice thickness. The DW signal decays were fitted monoexponentially to quantify the diffusivities in these phantoms. ***In vivo rat brain:*** A normal adult SD rat was anesthetized with isoflurane throughout the brain MRI experiment. A field-map based shimming technique (MAPSHIM, ParaVision5), in which field variations inside an ROI was compensated based on the static magnetic field distribution, was applied prior to diffusion experiment. The static magnetic field distribution was acquired with TR=20 ms, TE=1.96/8.62 ms and isotropic resolution (200μm). The shim volume was an 11x6 x1 mm^3 slab positioned in the rat brain and the resulting water linewidth was ~0.05 ppm. DW images were then acquired using the proposed DW-bSSFP sequence with the following parameters: TR/TE=46/23 ms, δ=10 ms, G=144 mT/m, b=1000 s/mm^2, α=30°, FOV=32 x 32 mm^2, acquisition matrix=128 X 128, slice thickness=1 mm NEX=16 and β=π. Diffusion encoded gradients were applied along 6 directions. For qualitative comparison, corresponding 8-shot SE-EPI DWIs were also acquired with the same slice localization, resolution and diffusion encoding directions (TR/TE=3200/28ms, δ/Δ=5/10 ms, b=1000 s/mm^2). All diffusion tensor image (DTI) maps were computed using the software DTIStudio. Note that, for DW-bSSFP, diffusivities along each direction were estimated by simply assuming the monoexponential DW signal decay with respect to b.

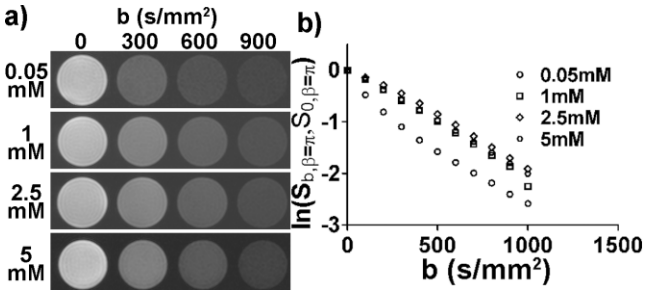

Fig. 3 a) B0 and diffusion weighted images (DWIs) of four Gd phantoms with different concentrations acquired at 7T using the proposed DW-bSSFP sequence . b) Plot of the normalized DW signal decay measurements from large ROIs within the phantoms, demonstrating the influence of Gd concentrations (i.e., relaxation times) on diffusion effect.

III. Results

The Gd phantom images without diffusion weighting (B_0) and DWIs acquired at 7T with different b-values are shown in Fig. 3a. No apparent distortion and ghosting artifacts were observed in these images. The DW signal attenuations in these phantoms are shown in Fig. 3b. Although the similar diffusivity value was found in these 4 phantoms using the DW-EPI protocol ($2.41\pm0.02\times10^{-3}$ mm^2/s), their DW-bSSFP signal decays were different. These experimental results clearly indicated that the DW-bSSFP decay characteristic is dependent of the relaxation times as predicted by the theoretical formulation above. Fig. 3b also shows that DW signal decay became increasingly mono-exponential when at large b-value (particularly after bD≥1). Note that the T_1 and T_2 ranges in these phantoms were estimated to be 50-1600 ms and 30-90 ms respectively, using SE sequence with varying TRs and multi-echo SE sequence.

Fig. 4a shows the rat brain B_0 images and DWIs acquired in vivo using the proposed DW-bSSFP and 8-shot respiratory-gated DW-EPI protocols. In white matter structures, DW-bSSFP images exhibited similar anisotropic information as that revealed by DW-EPI DWIs. No apparent head motion artifacts (associated with respiratory motion) and geometric distortions were observed in DW-bSSFP images. Note that ghosting artifacts were sometimes observed in DW-EPI images due to respiratory motion (not shown), but they were absent in all DW-bSSFP images acquired in the current study. Fig. 4b shows the DTI parametric maps that were computed from DW-bSSFP images by simply assuming monoexponential signal decay, which were qualitatively similar to those obtained by the DW-EPI protocol. Simple ROI measurements revealed that the diffusivities in most of brain regions differed quantitatively from those computed from DW-EPI images. This was largely expected given the complex signal attenuation behavior and the simple monoexponential model used in the diffusivity quantification from DW-SSFP signals. Some minor discrepancies in the FA maps were also observed. They likely arose from the actual non-monoexponential relationship between the measured diffusion attenuation and actual diffusivity. They might be also ascribed to the imperfect shimming and thus the resulting β (or more precisely, β_{B0}) effect, extent of which could vary with the actual diffusivity along any particular direction.

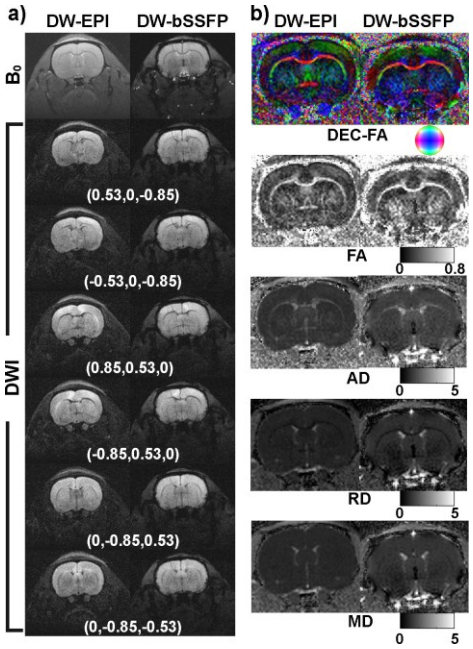

Fig. 4 a) B_0 and DWIs of an adult rat brain acquired in vivo at 7T using the proposed DW-bSSFP sequence and an 8-shot DW-EPI sequence. For each DWI, the diffusion encoding direction is shown within the image as (x, y, z). b) DTI parametric maps were computed from the DW-bSSFP and DW-EPI images, yielding qualitatively similar results. Diffusivities are in the unit of 10^{-3} mm^2/s. DEC-FA: directionally encoded FA; FA: fractional anisotropy; AD: axial diffusivity; RD: radial diffusivity; MD: mean diffusivity.

IV. Discussions and Conclusion

The diffusion effect in DW-bSSFP signal depends on not only the diffusivity and b-value, but also T_1, T_2 and acquisition sequence parameters, namely TR and flip angle. The major challenge of applying this DW-bSSFP is that the effects of these parameters have to be taken into account carefully during diffusivity quantification. Furthermore, the diffusion effect also depends on phase advance per TR(β) that can be incurred by both successive RF phase advance and magnetic field inhomogeneity, together with B_1 inhomogeneity that could affect the flip angle.

Several analytical and technical issues are yet to be resolved before the proposed DW-bSSFP approach produces efficient and robust diffusion quantification in practical applications. Given Eqs. 3 and 4, we need to measure T_1 and T_2 of each voxel to analytically quantify the diffusivity after obtaining the DW-bSSFP signals. In this regard, it remains to be addressed in the future studies how T_1 and T_2 measurement errors propagate into the diffusivity estimation so to determine the level of accuracy required for prior T_1 and T_2 knowledge. In practice, it may be possible to simplify these analytical equations presented. For example, with $TR<<T_1$ and β equal to 0 or π, the DW signal decays described by Eqs. 5 and 6 can be employed to measure diffusivity if only prior knowledge or estimation of T_2 is available. Also, note that DW bSSFP signal attenuation at large b values (2bD>1) varies with bD approximately in a simple monoexponential manner. The approaches to quantifying diffusivity using DW-bSSFP signals are yet to be evaluated and optimized for their accuracy and efficiency in practical applications. The

optimal approaches are expected to depend on field strength, acquisition sequence parameters, MRI system hardware capability and the relaxation property of the tissue targeted.

Technically, the vulnerability of DW-bSSFP images to static magnetic field inhomogeneity and magnetic susceptibility scales up with field strength and TR as in bSSFP imaging. It can be observed in Fig. 4a that both B_0 and DWIs exhibited certain signal loss or increase in some regions. This likely resulted from the varying β effect associated with the field inhomogeneity at 7T and the relatively long TR used (46 ms). Nevertheless, such bSSFP and DW-bSSFP image quality can be improved through improved shimming and use of shorter TR that can be achieved with increasingly available strong gradient and shimming hardware. Furthermore, the proposed DW-bSSFP approach can be particularly suitable to the MRI systems with low static field strength, good shimming and strong gradient.

DW-bSSFP approach can be utilized to quantify the diffusivity along any specific direction. Like other DW sequences, it can be generally applied to MR diffusion characterization of tissue microstructure and anisotropy via DTI or other higher order diffusion imaging[10, 11]. DW-bSSFP approach offers several advantages over the widely used DW-EPI approach. First, it allows high spatial resolution as a result of bSSFP acquisition. Because of the use of bipolar gradients with short diffusion time, the distortion due to eddy currents is expected to be minimal. Secondly, DW-bSSFP is less sensitive to the bulk motions that are relatively slow with respect to TR because of the fully balanced bipolar diffusion and imaging gradients, a distinct feature similar to that offered by standard bSSFP imaging. Therefore, the DW-bSSFP approach can be suited for diffusion imaging of the organs where motion insensitivity is required such as brain[12, 13], heart[14, 15], musculoskeletal system, spinal cord and other abdominal organs[16-18]. Furthermore, DW-bSSFP uses short diffusion time. Short diffusion time probes the complex and restricted diffusion processes with short diffusion distance, thus potentially offering different or/and more sensitive diffusion characterization of tissue microstructures because cellular compartments of different dimensions in may be better probed by choosing an appropriate diffusion distance. The diffusion gradient duration δ in Fig. 1 can be easily altered. However, the use of bipolar gradient also lengthens the TR that lead to a loss of SNR. Lastly, although only 2D DW-bSSFP was demonstrated in the current study, the formulation of diffusion effect in DW-bSSFP is equally applicable to 3D DW-bSSFP.

The diffusion effect in the proposed DW-bSSFP approach was formulated in analytically closed forms. The potential utility of DW-bSSFP to study neural tissue anisotropy was demonstrated in preliminary phantom and in vivo brain experiments. The proposed DW-bSSFP approach and analytical formulation presented can provide a new approach to diffusion imaging, including DTI, with high spatial resolution, minimal image distortion, relative motion insensitivity and short diffusion time. Such approach may lead to improved and new MR diffusion study of neural tissues and their microstructural characterization.

ACKNOWLEDGMENT

The work was in part supported by Hong Kong Research Grant Council and HKU CRCG grants.

REFERENCES

[1] P. Jezzard and R. S. Balaban, "Correction for geometric distortion in echo planar images from B0 field variations," *Magn Reson Med,* vol. 34, pp. 65-73, Jul 1995.

[2] R. Kaiser, E. Bartholdi, and R. R. Ernst, "Diffusion and field-gradient effects in NMR Fourier spectroscopy," *The Journal of Chemical Physics,* vol. 60, pp. 2966-79, 1974.

[3] E. X. Wu and R. B. Buxton, "Effect of Diffusion on the Steady-State Magnetization with Pulsed Field Gradients," *Journal of Magnetic Resonance,* pp. 243-53, 1990.

[4] J. A. McNab and K. L. Miller, "Sensitivity of diffusion weighted steady state free precession to anisotropic diffusion," *Magn Reson Med,* vol. 60, pp. 405-13, Aug 2008.

[5] O. Bieri, C. Ganter, G. H. Welsch, S. Trattnig, T. C. Mamisch, and K. Scheffler, "Fast diffusion-weighted steady state free precession imaging of in vivo knee cartilage," *Magn Reson Med,* vol. 67, pp. 691-700, Mar 2012.

[6] J. A. McNab, S. Jbabdi, S. C. Deoni, G. Douaud, T. E. Behrens, and K. L. Miller, "High resolution diffusion-weighted imaging in fixed human brain using diffusion-weighted steady state free precession," *Neuroimage,* vol. 46, pp. 775-85, Jul 1 2009.

[7] S. Ding, H. Trillaud, M. Yongbi, E. L. Rolett, J. B. Weaver, and J. F. Dunn, "High resolution renal diffusion imaging using a modified steady-state free precession sequence," *Magn Reson Med,* vol. 34, pp. 586-95, Oct 1995.

[8] Y. Zur, M. L. Wood, and L. J. Neuringer, "Motion-insensitive, steady-state free precession imaging," *Magn Reson Med,* vol. 16, pp. 444-59, Dec 1990.

[9] H. Y. Carr, "Steady-state free precession in nuclear magnetic resonance," *Phys Rev,* vol. 112, pp. 1693-701, 1956.

[10] E. X. Wu and M. M. Cheung, "MR diffusion kurtosis imaging for neural tissue characterization," *NMR in biomedicine,* vol. 23, pp. 836-48, Aug 2010.

[11] E. S. Hui, M. M. Cheung, K. C. Chan, and E. X. Wu, "B-value dependence of DTI quantitation and sensitivity in detecting neural tissue changes," *NeuroImage,* vol. 49, pp. 2366-74, Feb 1 2010.

[12] K. C. Chan, P. L. Khong, H. F. Lau, P. T. Cheung, and E. X. Wu, "Late measures of microstructural alterations in severe neonatal hypoxic-ischemic encephalopathy by MR diffusion tensor imaging," *International journal of developmental neuroscience,* vol. 27, pp. 607-15, Oct 2009.

[13] K. C. Chan, P. L. Khong, M. M. Cheung, S. Wang, K. X. Cai, and E. X. Wu, "MRI of late microstructural and metabolic alterations in radiation-induced brain injuries," *Journal of magnetic resonance imaging : JMRI,* vol. 29, pp. 1013-20, May 2009.

[14] E. X. Wu, Y. Wu, H. Tang, J. Wang, J. Yang, M. C. Ng, E. S. Yang, C. W. Chan, S. Zhu, C. P. Lau, and H. F. Tse, "Study of myocardial fiber pathway using magnetic resonance diffusion tensor imaging," *Magn Reson Imaging,* vol. 25, pp. 1048-57, Sep 2007.

[15] Y. Wu, C. W. Chan, J. M. Nicholls, S. Liao, H. F. Tse, and E. X. Wu, "MR study of the effect of infarct size and location on left ventricular functional and microstructural alterations in porcine models," *Journal of magnetic resonance imaging : JMRI,* vol. 29, pp. 305-12, Feb 2009.

[16] J. S. Cheung, S. J. Fan, A. M. Chow, E. S. Hui, and E. X. Wu, "In vivo DTI assessment of hepatic ischemia reperfusion injury in an experimental rat model," *Journal of magnetic resonance imaging : JMRI,* vol. 30, pp. 890-5, Oct 2009.

[17] J. S. Cheung, S. J. Fan, A. M. Chow, J. Zhang, K. Man, and E. X. Wu, "Diffusion tensor imaging of renal ischemia reperfusion injury in an experimental model," *NMR in biomedicine,* vol. 23, pp. 496-502, Jun 2010.

[18] J. S. Cheung, S. J. Fan, D. S. Gao, A. M. Chow, K. Man, and E. X. Wu, "Diffusion tensor imaging of liver fibrosis in an experimental model," *Journal of magnetic resonance imaging : JMRI,* vol. 32, pp. 1141-8, Nov 2010.